

Microsphere Manipulation Using Ferroelectric Liquid Crystals

Yoshitaka Mieda* and Katsushi Furutani

Department of Advanced Science and Technology, Toyota Technological Institute,
12-1 Hisakata 2-chome, Tempaku-ku, Nagoya 468-8511, Japan

(Received 23 June 2005; published 20 October 2005)

We propose a strategy for a micromanipulation method using SSFLC (surface stabilized ferroelectric liquid crystals). By adjusting the frequency of the applied ac electric field, the surface layers that cannot follow an applied ac electric field are constructed in SSFLC. In addition, by applying a sawtooth wave voltage, net flow along the smectic layer is generated. The flow direction is reversed by changing the polarity of the sawtooth wave. Consequently, the particles dispersed in SSFLC can be driven bidirectionally along the smectic layer. The particle velocity depends on the temperature, amplitude, and frequency of the applied voltage.

DOI: [10.1103/PhysRevLett.95.177801](https://doi.org/10.1103/PhysRevLett.95.177801)

PACS numbers: 61.30.-v, 61.30.Dk, 61.30.Gd

Recently, solid or liquid micro- or nanoparticle dispersions in liquid crystals (LCs) have attracted interest [1–6]. The static interactions between the LCs and the dispersed particles were first studied [1]. The main interests then shifted to the dynamic interactions [2,3]. In addition, the manipulation of dispersed particles was studied [4,5]. We also reported a two-dimensional micromanipulation method using the backflow effect generated in a twisted nematic cell [6]. These manipulation methods are expected to be applied to biochips and μ -TAS (micrototal analysis systems) [7] in the future.

These topics are related to nematic or lyotropic LCs. The particle dispersed smectic LCs have barely been studied because smectic systems are more complex than the nematic or lyotropic ones. Until now, it has been reported that the dispersed particles in the surface stabilized ferroelectric liquid crystals (SSFLC) migrated along the smectic layer by applying a voltage [8]. The origin of this migration is the backflow effect [9] or electromechanical vibration [10]. However, the motion of the dispersed particles cannot yet be controlled. In this Letter, to manipulate the dispersed particles in smectic systems, we propose a strategy based on the backflow effect in SSFLC and experimentally verify it.

Figure 1 shows the principle of the micromanipulation method using SSFLC. By rubbing in the same direction on both substrates, the c directors (the projection of the n directors on the smectic layer) are symmetrically aligned in the y direction as shown in Fig. 1(a). This state is analogous to the π -cell alignment in the nematic LCs [11]. Here, let us consider the flow generated by the switching while applying a sawtooth electric field. In the transient part of the sawtooth wave, because the direction of the electric field rapidly changes, the local spontaneous polarization (P_s) is rapidly aligned parallel to the electric field [Fig. 1(b)]. For conventional SSFLC devices, the switching of surface layers is necessary for the appearance of the bistability. However, in our strategy, the key element is the existence of surface layers that do not switch. These sur-

face layers are easily made by adjusting the frequency of the applied ac electric field (the surface anchoring and applied field strength also affect the existence of the surface layers). As a result, the backflow represented by U_x is generated. On the other hand, at the slope portions of the sawtooth wave [Fig. 1(c)], the c director alignment gradually returns to the initial state [Fig. 1(a')]. In this case, the backflow in the reverse direction is generated. However, because the alignment slowly changes, only a weak flow is generated as shown in a later calculation. Therefore, a net flow is generated and the microparticles mixed in the LCs are driven in the $-x$ direction. Next, we reverse the polarity of the sawtooth wave. In this case, the bistable switching discussed in Ref. [12] occurs, and the net flow in the $+x$ direction is generated in the same way described in Fig. 1. Therefore, by reversing the polarity of the ac sawtooth wave, the particles can be driven bidirectionally along the smectic layer.

Here, based on a numerical calculation, we analyzed the flow generated by applying a sawtooth wave voltage. To analyze this phenomenon, the LSN (Leslie, Stewart, Nakagawa) theory, which is the complex continuum theory for SmC^* [13,14], is not necessary. It is only necessary to

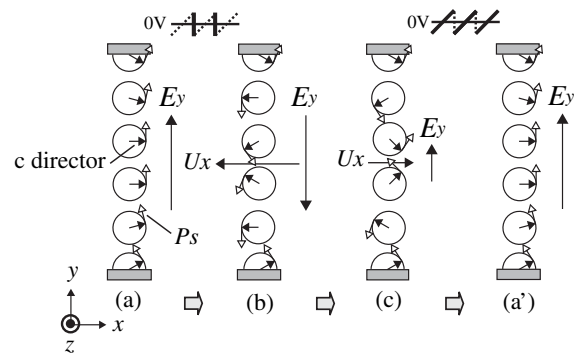


FIG. 1. The principle of a micromanipulation method using SSFLC. The z axis represents the layer normal and the rubbing direction. Bookshelf geometry is assumed.

use the nematodynamic analog. Since the c director and flow velocity are restricted in the x - y plane and x direction, respectively, the dynamic behavior of the system is expressed [15] by

$$\rho \frac{\partial U_x}{\partial t} = \frac{\partial}{\partial y} \left\{ g \frac{\partial U_x}{\partial y} + m \frac{\partial \phi}{\partial t} \right\}, \quad (1)$$

$$0 = \Gamma - \gamma_1^c \frac{\partial \phi}{\partial t} - m \frac{\partial U_x}{\partial y}, \quad (2)$$

where ρ is the mass density, $U_x = U_x(y, t)$ is the x directional component of the flow velocity, $\phi = \phi(y, t)$ is the tilt angle of the c director from the x axis, and g and m are the effective shear viscosity coefficient and the effective shear-torque coupling coefficient, respectively. Γ represents $\Gamma_{\text{elect}} + \Gamma_{\text{elas}}$, where Γ_{elect} and Γ_{elas} are the electric and elastic torques for c director, respectively. The g and m are written as

$$g = \eta_2^c \cos^2 \phi + \eta_1^c \sin^2 \phi + \eta_{12}^c \sin^2 \phi \cos^2 \phi, \quad (3)$$

$$m = \frac{\gamma_1^c + \gamma_2^c}{2} \cos^2 \phi + \frac{\gamma_1^c - \gamma_2^c}{2} \sin^2 \phi, \quad (4)$$

where η_1^c , η_2^c , η_{12}^c are the Mięsiowicz constants, and γ_1^c , γ_2^c are the rotational viscosity coefficients [16]. On the other hand, Γ_{elas} and Γ_{elect} are written as

$$\Gamma_{\text{elect}} = -P_s E_y \sin \phi, \quad (5)$$

$$\Gamma_{\text{elas}} = (k_1^c \cos^2 \phi + k_3^c \sin^2 \phi) \frac{\partial^2 \phi}{\partial y^2} + \frac{1}{2} (k_3^c - k_1^c) \sin 2\phi \left(\frac{\partial \phi}{\partial y} \right)^2, \quad (6)$$

where E_y is the y component of the electric field, and k_1^c and k_3^c are elastic constants. The dielectric torque was neglected.

Figure 2 shows the calculated results using the Crank-Nicholson method. Because most of the material parameters of the FLCs were not experimentally obtained, we assumed that they were almost the same as the nematic LCs, and used the following values: $\eta_1^c = \eta_2^c \approx 10^{-1}$ Pa s, $\eta_{12}^c = 0$, $\gamma_1^c \approx 10^{-3}$ Pa s, $\gamma_2^c = \eta_2^c - \eta_1^c = 0$, $k_1^c = k_3^c \approx 10^{-11}$ N. The others are shown in the caption of Fig. 2. As illustrated in Fig. 2(a), one cycle of the sawtooth wave (1 kHz) was used as the applied voltage V . E_y is calculated by V/d , where d represents the cell gap length. Figure 2(b) shows the time dependence of the c director distribution. Because the surface layer does not switch in the system, we used $\phi(0, t) = 1^\circ$, $\phi(d, t) = -1^\circ$ as the boundary conditions. The initial condition was derived from Eq. (2) with the field strength at $t = 0$ and $\partial \phi / \partial t = \partial U_x / \partial y = 0$. After a cycle, the condition of the cell returned to the initial state. Figure 2(c) shows time dependence of the flow velocity distribution. We assumed

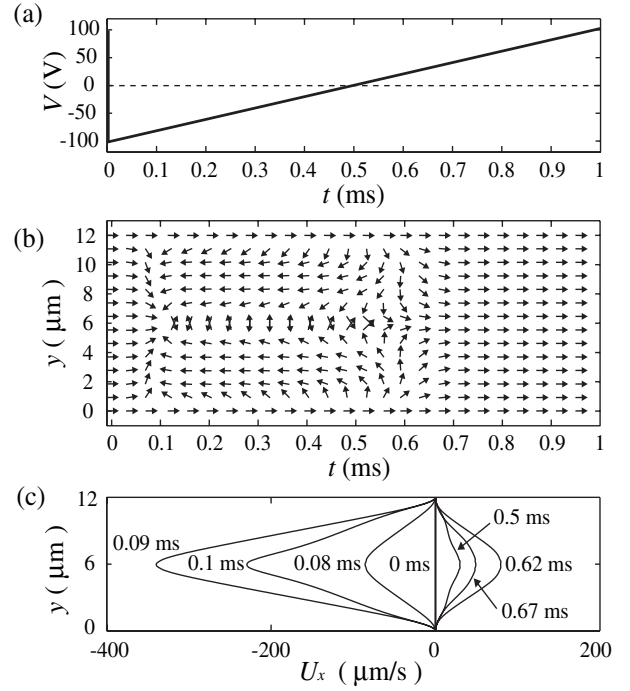


FIG. 2. Results of numerical calculation. (a) Applied sawtooth wave. (b) Time dependence of c director distribution. The arrows represent the c director. For simplification, a strong anchoring was applied to the boundary conditions. (c) Time dependence of flow velocity distribution. In these calculations, the following parameters were used: $\rho = 10^3$ kg/m³, $P_s = +10$ $\mu\text{C}/\text{m}^2$, $d = 12$ μm .

$U_x(0, t) = U_x(d, t) = 0$ as the boundary conditions and $U_x(y, 0) = 0$ as the initial condition. As shown in Fig. 2(c), the flow in the $-x$ direction is stronger than the flow in the $+x$ direction. Therefore, a net flow in the $-x$ direction occurs.

In order to check the performance of the micromanipulation method, the following experiments were carried out. Two glass substrates with an indium-tin-oxide electrode were spin coated with polyimide (RN-1199, from Nissan Chemical Industry Ltd.), rubbed by the cloth, and glued together with the 12 μm polyethylene terephthalate spacers. The electrode area measured 10 mm \times 10 mm. As the FLC and microparticles, FELIX-015/000 [SmC^* 71 $^\circ\text{C}$ SmA 83 $^\circ\text{C}$ N^* 86–83 $^\circ\text{C}$ I , from Clariant (Japan) K. K.] and the spherical polymer beads with a diameter of 10 μm (Micropearl SP, from Sekisui Chemical Co., Ltd.) were used, respectively. By capillarity in the isotropic phase, the FLC mixed with the polymer beads were injected into the cell, and then the single domain SSFLC structure was obtained by a cooling process.

Measurements were performed by applying a sawtooth wave voltage through an amplifier from the function generator. The temperature of the LC cell was controlled using an oven. The motion of the particles was observed using a video microscope and recorded on a videocassette recorder

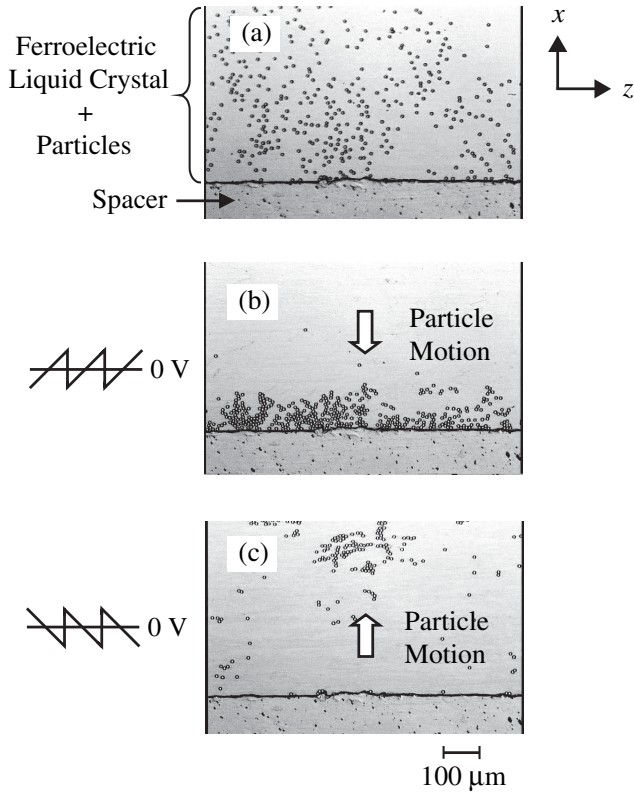


FIG. 3. Microphotographs of the particle motion. (a) The initial dispersion with no applied voltage. (b) The $-x$ directional motion. (c) The $+x$ directional motion. The microspheres were contingently adsorbed on the substrates. Therefore, the drift velocities were measured by selecting the arbitrary spheres not adsorbed on the substrates. However, these adsorptions were sometimes negated by the flow; (b) is a photograph for the flow applied for a time longer than (c).

for motion analysis. Figure 3 shows the change in the particles motion when reversing the sawtooth wave polarity. Figure 3(a) shows the initial state with no applied voltage. When the sawtooth wave, shown in Fig. 3(b), was applied, the particles moved in the $-x$ direction. On the other hand, when the sawtooth wave polarity was reversed as shown in Fig. 3(c), the particles moved in the $+x$ direction.

Figure 4 shows the frequency f dependence on the particle velocity U . The temperature and the amplitude of the sawtooth wave were fixed at 66°C and 80 V , respectively. U was obtained by averaging the traveling distance for five particles in 10 s . At $f < 1\text{ kHz}$, because the breaking of the surface anchoring disturbs the generation of the net flow, the particles could not move. At $f > 1\text{ kHz}$, the particles moved and U increased with the increase in f . However, at $f > 4\text{ kHz}$, U decreased, because the slope portion of the sawtooth wave became too steep in the higher frequency region; it can be considered that a rectangular wave was applied, and the flows generated in the transient part and slope of the sawtooth wave

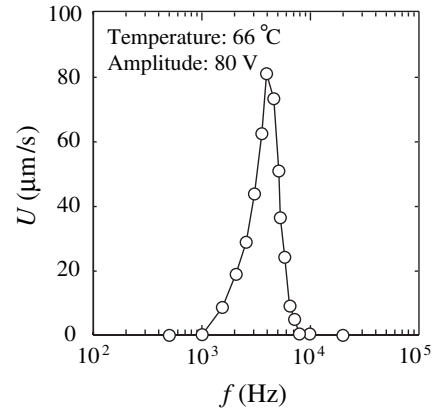


FIG. 4. Frequency dependence of the particle velocity.

canceled each other out. At $f > 10\text{ kHz}$, the particles could not move at all, because the ferroelectric switching hardly followed the change in the ac electric field at high frequency. Though the data are not shown in the figure, the particles moved at $f < 10\text{ Hz}$ equivalent to dc voltage. This unusual phenomenon was due to the unstable flows based on the conductivity of the ionic impurities.

Figure 5 shows the temperature T dependence of U . The frequency and amplitude of the applied voltage were fixed at 4 kHz and 80 V , respectively. U peaked at $T = 66^\circ\text{C}$. At $T < 60^\circ\text{C}$, the particles could not move. This was attributed to the increasing viscosity. On the other hand, the decreasing the drift velocity near T_C originated from the attenuation of P_s and the tilt angle θ of the n director. At $T > 71^\circ\text{C}$, the particles did not move at all, because the phase transition to SmA occurred.

Figure 6 shows the voltage amplitude V dependence of U . The f and T values were fixed at 4 kHz and 66°C , respectively. The particles did not move below a threshold voltage ($V = 40\text{ V}$), because the net flow was weak at the low voltage and the adsorption force by the substrates was greater than the force by the backflow. At $V > 40\text{ V}$, the

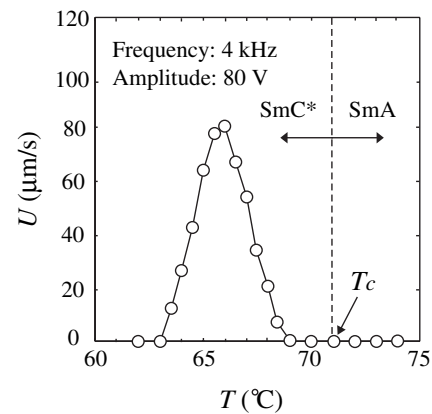


FIG. 5. Temperature dependence of the particle velocity. T_C represents the Curie temperature for the SmC * -SmA phase transition.

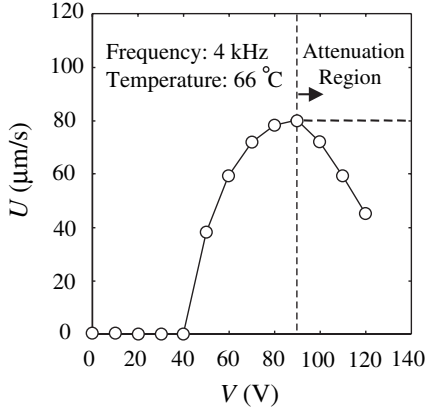


FIG. 6. Amplitude dependence of the particle velocity.

particles moved and U peaked at $V = 90$ V. Above $V = 90$ V, U became small. This was because, at a constant frequency, the slope part of the sawtooth wave became steep when the amplitude increased. At $V > 120$ V, measurements became difficult, because the electric discharge often occurred.

We proposed a strategy for the particle micromanipulation method using SSFLC. By applying the sawtooth wave voltage, a net movement of the particles along the smectic layer was generated. Moreover, the movement direction was able to be reversed by changing the polarity of the sawtooth wave. The particle velocity depended on the temperature, amplitude, and frequency of the applied voltage.

This research was partially supported by the Ministry of Education, Science, Sports, and Culture, Grant-in-Aid for Scientific Research on Young Scientists (B) (17760124).

*Electronic address: mieda@toyota-ti.ac.jp

- [1] P. Poulin, H. Stark, T.C. Lubensky, and D.A. Weitz, *Science* **275**, 1770 (1997).
- [2] J.C. Loubet, P. Hanusse, and P. Poulin, *Science* **306**, 1525 (2004).
- [3] J. Yamamoto and H. Tanaka, *Nat. Mater.* **4**, 75 (2005).
- [4] J.L. West, A. Glushchenko, G. Liao, Yu. Reznikov, D. Andrienko, and M.P. Allen, *Phys. Rev. E* **66**, 012702 (2002).
- [5] I.I. Smalyukh, A.N. Kuzmin, A.V. Kachynski, P.N. Prasad, and O.D. Lavrentovich, *Appl. Phys. Lett.* **86**, 021913 (2005).
- [6] Y. Mieda and K. Furutani, *Appl. Phys. Lett.* **86**, 101901 (2005).
- [7] R.R. Shah and N. Abbott, *Science* **293**, 1296 (2001).
- [8] T. Togo, K. Nakayama, M. Ozaki, and K. Yoshino, *Jpn. J. Appl. Phys. Part 2* **36**, L1520 (1997).
- [9] Z. Zou and N. Clark, *Phys. Rev. Lett.* **75**, 1799 (1995).

- [10] A. Jákli, L. Bata, Á. Buka, N. Éber, and J. Jánossy, *J. Phys. (Paris)* **46**, L759 (1985).
- [11] P.J. Bos and K.R. Koehler/Beran, *Mol. Cryst. Liq. Cryst.* **113**, 329 (1984).
- [12] J.E. MacLennan, M.A. Handschy, and N.A. Clark, *Liq. Cryst.* **7**, 787 (1990).
- [13] F.M. Leslie, I.W. Stewart, and M. Nakagawa, *Mol. Cryst. Liq. Cryst.* **198**, 443 (1991).
- [14] Z. Zou, N.A. Clark, and T. Carlsson, *Jpn. J. Appl. Phys.* **34**, 560 (1995).
- [15] See, e.g., P. Pieranski, F. Brochard, and E. Guyon, *J. Phys. (Paris)* **34**, 35 (1973); M.G. Clark and F.M. Leslie, *Proc. R. Soc. A* **361**, 463 (1978). We regarded the tilt angle θ of the n director in their article as the tilt angle ϕ of the c director.
- [16] These parameters are connected with the parameters of the LSN theory as follows. Now, η_1^c , η_2^c , η_{12}^c are written as

$$\eta_1^c = \frac{1}{2}(-\alpha_2^c + \alpha_4^c + \alpha_5^c), \quad (7)$$

$$\eta_2^c = \frac{1}{2}(\alpha_3^c + \alpha_4^c + \alpha_6^c), \quad (8)$$

$$\eta_{12}^c = \alpha_1^c, \quad (9)$$

by six Leslie coefficients. γ_1^c and γ_2^c are written as

$$\gamma_1^c = \alpha_3^c - \alpha_2^c, \quad (10)$$

$$\gamma_2^c = \alpha_6^c - \alpha_5^c. \quad (11)$$

Here, we substitute $2\lambda_2$ on both sides of Parodi's relation,

$$\alpha_2^c + \alpha_3^c = \alpha_6^c - \alpha_5^c. \quad (12)$$

The λ_2 value is an arbitrary real number. Moreover, by introducing two arbitrary real numbers, μ_4 and λ_5 , Eq. (12) is divided into

$$\alpha_2^c = \lambda_2 - \lambda_5, \quad (13)$$

$$\alpha_3^c = \lambda_2 + \lambda_5, \quad (14)$$

$$\alpha_5^c = \mu_4 - \lambda_2, \quad (15)$$

$$\alpha_6^c = \mu_4 + \lambda_2. \quad (16)$$

In addition, let arbitrary real numbers μ_3 and μ_0 be the remaining α_1^c and α_4^c , respectively;

$$\alpha_1^c = \mu_3, \quad (17)$$

$$\alpha_4^c = \mu_0. \quad (18)$$

By using the relations of Eqs. (7)–(11) and substituting Eqs. (13)–(18) into Eqs. (3) and (4), we obtain

$$g = \frac{1}{2}\mu_0 + \frac{1}{2}\mu_4 + \mu_3 \sin^2 \phi \cos^2 \phi + \lambda_2 \cos 2\phi + \frac{1}{2}\lambda_5, \quad (19)$$

$$m = \lambda_2 \cos 2\phi + \lambda_5. \quad (20)$$

Equations (19) and (20) agree with the viscosity torque derived by the LSN theory in Ref. [14].